VISRAD Benchmark Calculation:
OMEGA Capsule Radiation Symmetry

In this *VISRAD* benchmark calculation, we compare *VISRAD* hohlraum radiation symmetry calculations with measurements obtained in OMEGA experiments. The OMEGA data are based on results reported by Murphy *et al.* (Phys. Rev. Lett. **81**, 108, 1998). Hohlraum and capsule dimensions, as well as laser beam energies and pointings, are based on the Murphy *et al.* paper.

In these indirect-drive experiments, up to 40 of the 60 OMEGA laser beams enter the hohlraum laser entrance holes (LEHs). The beams are arranged in 3 cones, with entrance angles (*i.e.*, half-cone angles) of 21.42°, 42.02°, and 58.85° for Cones 1, 2, and 3, respectively. The pointing[1] of the cones was adjusted in a series of 3 experimental scans to assess the effects of the beam pointing on the capsule radiation asymmetry. The asymmetry of the incident radiation flux onto the capsule was inferred in the experiments from imploded core images, which recorded emission originating from argon contained within the capsule. The shape of the core image was measured in the experiments, and parameterized by the ratio of the radius perpendicular to the hohlraum axis, *a*, to that parallel to the hohlraum axis, *b*.

In each of the experiments, the radius of the hohlraum was 800 μm and the LEH radius was 600 μm. The capsule radius was 275 μm. Each of the laser beams had a nominal energy of 500 J in a 1 ns flat-topped laser pulse.

The main adjustable parameters in the three experimental series are summarized in Table 1. The experiments are grouped in a manner similar to that shown in Figure 3 of the Murphy *et al.* paper.

Table 1. Summary of parameters adjusted in Murphy *et al.* experiments.

Experiment	Hohlraum length (μm)	Cone 1 Pointing (μm)	Cone 2 Pointing (μm)	Cone 3 Pointing (μm)
A-1	2500	off	1500	1200
A-2	2300	off	1400	1100
A-3	2100	off	1300	1000
B-1	2500	off	1500	1200
B-2	2500	off	1300	1200
B-3	2500	off	1100	1200
C-1	2500	off	1500	1200
C-2	2500	1300	1500	1200
C-3	2500	1500	1500	1200

In the *VISRAD* simulations, we used the experimental parameters discussed above. A screendump showing the beams from each of the three cones entering one of the hohlraum LEHs is shown in Figure 1. For each of the different laser pointings, the incident radiation flux onto the capsule is computed, and the asymmetry of the radiation field is examined. The asymmetry of the radiation flux is then compared with the *a/b* ratios from the experimental imploded core images.

[1] "Pointing" is defined as the distance from the center of the hohlraum to the point where the beams cross the hohlraum axis.

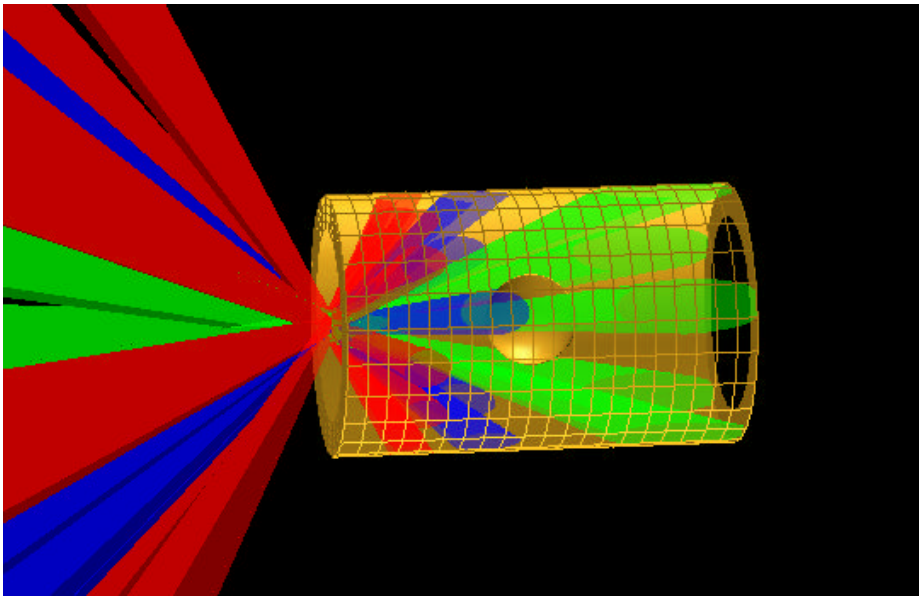

Figure 1. *VISRAD* screenshot showing beams of Cone 1 (green), Cone 2 (blue), and Cone 3 (red) entering one of the hohlraum LEHs. In this illustration, the beams are pointed such that the focus is at the center of the LEH.

The asymmetry of the radiation flux on the capsule is time-dependent. This can occur due to time-dependent hohlraum wall albedos, laser pulse shapes (though in the Murphy *et al*. experiments, 1 ns flat-topped pulses were used), and laser spot motion due to plasma ablated off the hohlraum wall. In these simulations, we take advantage of *VISRAD's* ability to model time-dependent quantities. The time-dependent hohlraum albedos and x-ray conversion efficiencies utilized in the simulations are the same as those used in the *VISRAD* calculations of OMEGA hohlraum radiation temperatures (see appendix in *VISRAD* documentation "Benchmark Calculation: OMEGA Hohlraum Temperatures"). These albedos and x-ray conversion efficiencies are shown in Figures 2 and 3.

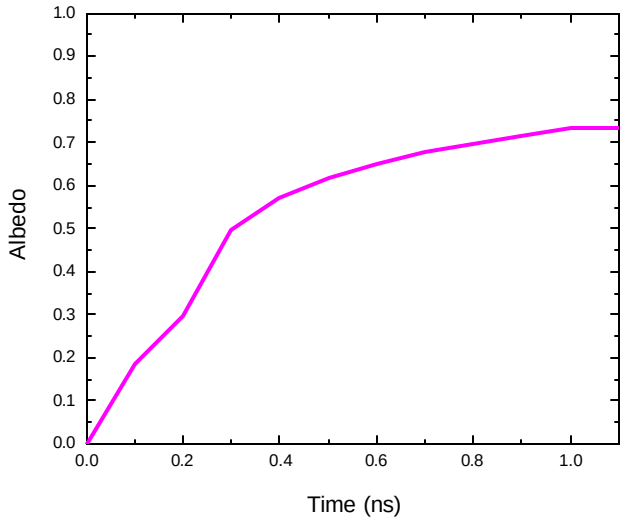

Figure 2. Albedo vs. time used in the *VISRAD* simulations. Albedos were obtained from a *HELIOS* 1-D radiation-hydrodynamics simulation of a radiation-driven Au foil.

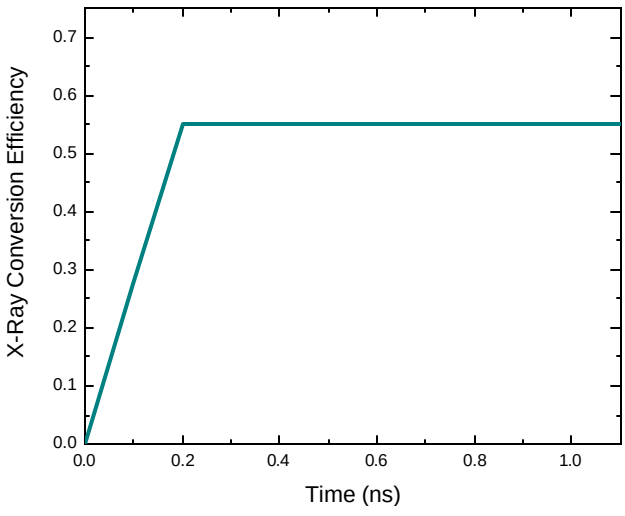

Figure 3. X-ray conversion efficiency vs. time used in the *VISRAD* simulations.

In the *VISRAD* simulations, the hohlraum was aligned along the P6 - P7 axis, and the capsule was oriented so that its poles were aligned with the hohlraum axis. The "glint" option was turned off (*i.e.*, there was no specular reflection of laser light). The view factor grid was composed of a total of 1080 surface elements.

Results from *VISRAD* calculations are shown in Figures 4 through 6. Figure 4 shows an image exported from *VISRAD* showing a color contour of the incident radiation flux onto the capsule for Case A-1 (note that Case A-1 is identical to B-1 and C-1). From the figure, it is clearly seen that there is very little variation in flux in the azimuthal direction, while the variation with polar angle can be substantial.

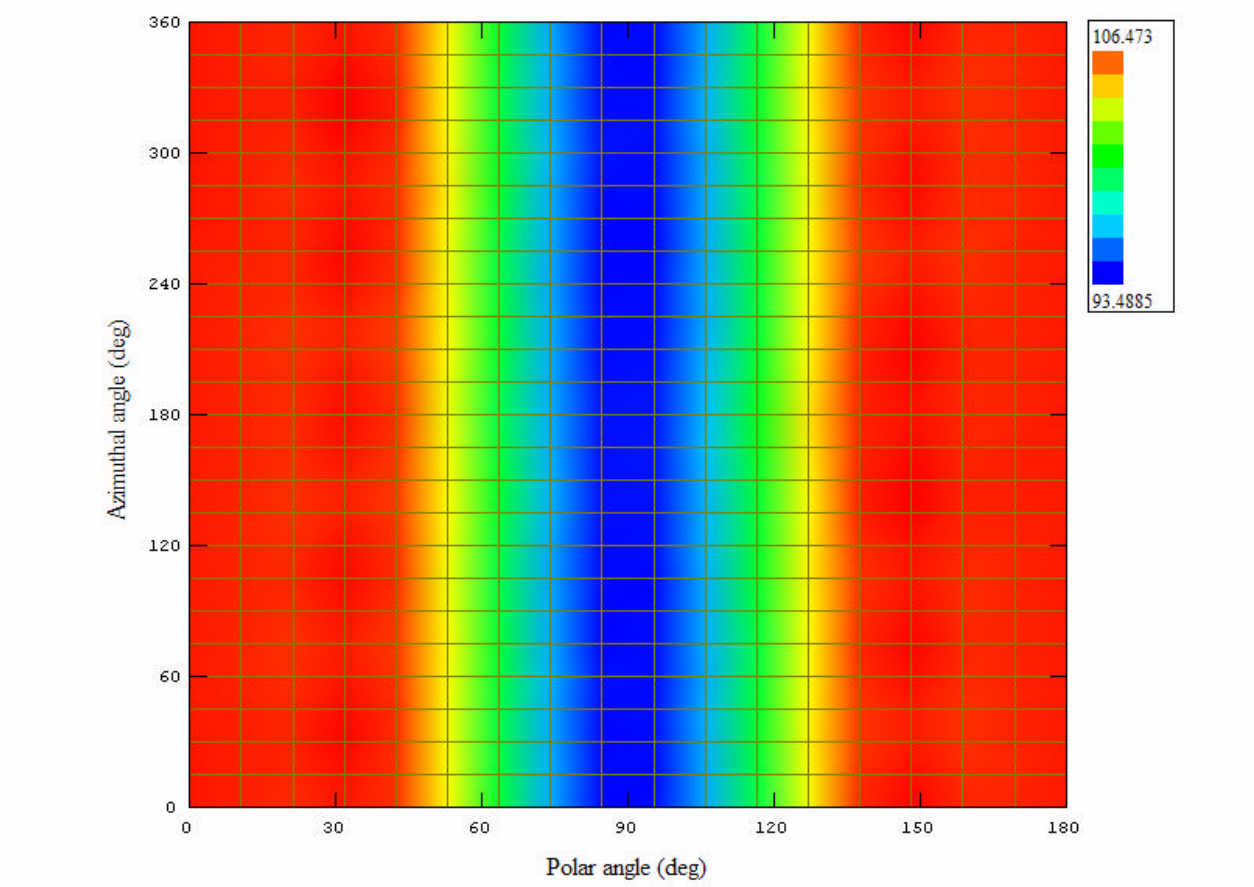

Figure 4. Calculated incident radiation flux onto the capsule for Case A-1 as a function of capsule azimuthal angle and polar angle. Results correspond to a time of 0.5 ns.

Results for the distribution of radiation flux incident on the capsule were fitted, within the *VISRAD* simulation, to an expansion in Legendre polynomials:

$$F_i = \sum_{\ell} a_\ell \; P_\ell(\cos q)\,,$$

where a_ℓ are coefficients (obtained from fitting), P_ℓ are Legendre polynomials, and q is the polar angle. For this study, the expansion was limited to $\ell_{\max} = 2$. Values of (a_2/a_0) from the *VISRAD* simulations are compared with the measured (a/b) ratios obtained from the experimental core images. Note that when the incident flux is symmetric, a_2/a_0 is zero.

Figure 5 shows the computed P_2 Legendre coefficient, normalized to the P_0 coefficient (*i.e.*, the mean incident flux, a_0) as a function of time for each of the cases listed in Table 1. Results from these baseline simulations, which do not include wall motion, are shown as solid curves. The value of the P_2 coefficient varies with time in a given simulation because the hohlraum albedo is time-dependent. For Case A-1 (as well as B-1 and C-1), the value of a_2/a_0 is everywhere positive. This means the flux at the poles is greater than the flux at the equator (as is shown in Figure 4). This *pole-hot* situation will produce a compressed capsule that has an *a/b* ratio > 1; that is, the capsule radius perpendicular to the hohlraum axis, *a*, is greater than the radius parallel to the hohlraum axis, *b*.

An additional series of *VISRAD* simulations was performed in which the hohlraum radius decreased with time to mimic the effect of the motion of laser hot spots, which occurs as plasma from the hohlraum wall ablates inward toward the hohlraum axis. This series of calculations was done to assess the potential effects of hot spot motion on the capsule radiation asymmetry. Here, we simply assume the radius of the hohlraum wall decreases by 100 μm (or 12.5% of the original radius) over the 1 ns laser pulse. Results for a_2/a_0 for this set of simulations are shown as dashed lines in Figure 5.

The effect of wall motion is seen to increase the value of a_2/a_0 with time. For the Case A and Case B series, the effect is seen to be fairly substantial. For the Case C series (variation in Cone 1 pointing) the effects are seen to be less pronounced.

Figure 6 shows *time-averaged* values of a_2/a_0 for each of the simulations in Table 1. Results from calculations with no wall motion are represented by the blue squares, while those with wall motion are represented by the red squares. The results can be compared with the experimental determinations of Murphy *et al*. shown in Figure 7. For the Case A series – in which beam Cones 2 and 3 form a single ring on each side of the hohlraum and the hohlraum length was varied – the *a/b* ratio in the experiments crosses from less than 1 to greater than 1 at a Cone 2 pointing of about 1370 μm (see Figure 7(a)). In the *VISRAD* simulations, the P_2 coefficient crosses from negative to positive at a Cone 2 pointing of 1430 μm and 1370 μm for the stationary wall and wall motion cases, respectively. That is, the simulations predict the capsule radiation transitions from *equator-hot* to *pole-hot* at a Cone 2 pointing that is in good agreement with experimental measurements.

Similar results are seen for the Case B series, in which the pointing of Cone 2 was varied while that of Cone 3 remained fixed at 1200 μm. In this case, the *a/b* ratio in the experiments crosses from less than 1 to greater than 1 at a Cone 2 pointing of about 1200 μm. In the *VISRAD* simulations, the P_2 coefficient crosses from negative to positive at a Cone 2 pointing of 1330 μm and 1280 μm for the stationary wall and wall motion cases, respectively. Again, the agreement between simulation and experiment is found to be reasonably good.

For the Case C series – in which Cone 1 was added while Cones 2 and 3 remained fixed at 1500 μm and 1200 μm, respectively – inclusion of Cone 1 reduces the asymmetry in both experiment and simulation. In the 1300 μm pointing case, both experiment and simulation exhibit pole-hot results, with the asymmetry being less than the case in which Cone 1 beams are turned off. In the 1500 μm pointing case, the experiment exhibits pole-hot results similar to the 1300 μm pointing case, while the simulation shows a more symmetric result.

Conclusions

In this series of simulations of OMEGA capsule radiation symmetry experiments, the *VISRAD* results are found to be in good general agreement with experimental measurements. The calculated dependence of the capsule radiation asymmetry on the pointing of laser beam cones is consistent with experimental imploded core image data reported by Murphy *et al.*

In addition, it is found that hohlraum wall motion can exhibit a notable change in the (time-dependent) symmetry of the radiation flux onto the capsule. While multi-dimensional radiation-hydrodynamics simulations can be performed to study the effects of wall motion and the dynamics of imploded cores in substantial detail, *VISRAD* simulations can provide – with modest effort – very reasonable estimates of the 3-D radiation field (asymmetries and temperatures) throughout ICF hohlraums.

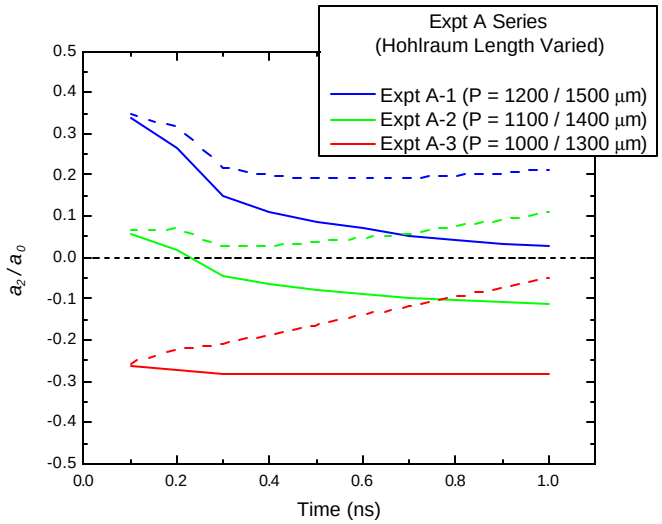

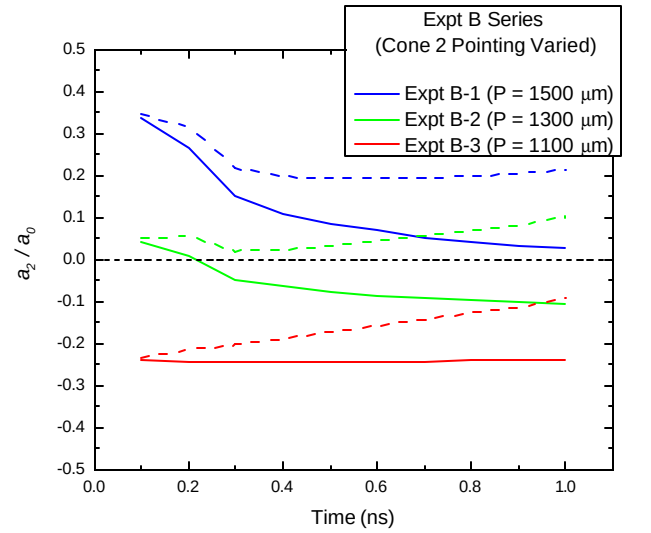

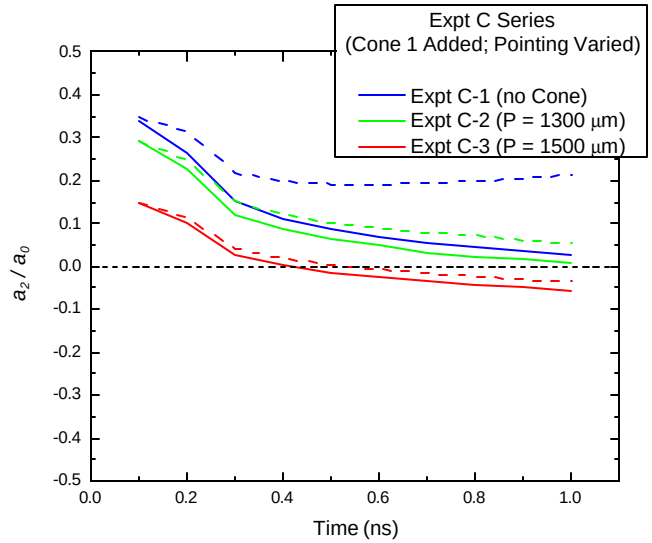

Figure 5. Calculated ratio of Legendre coefficients, a_2/a_0, as a function of time for all cases in Table 1. Solid curves: stationary wall calculations. Dashed curves: time-dependent hohlraum size calculations.

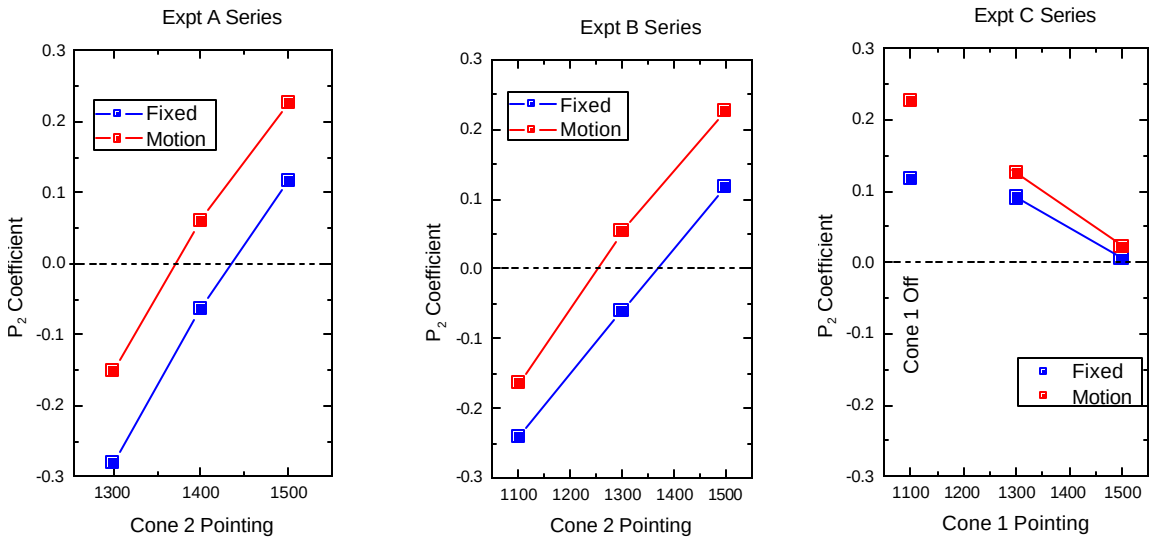

Figure 6. Time-averaged values of the normalized P_2 coefficient, a_2/a_0, from *VISRAD* simulations. Blue: results from simulation with no wall motion. Red: results from simulations with wall motion.

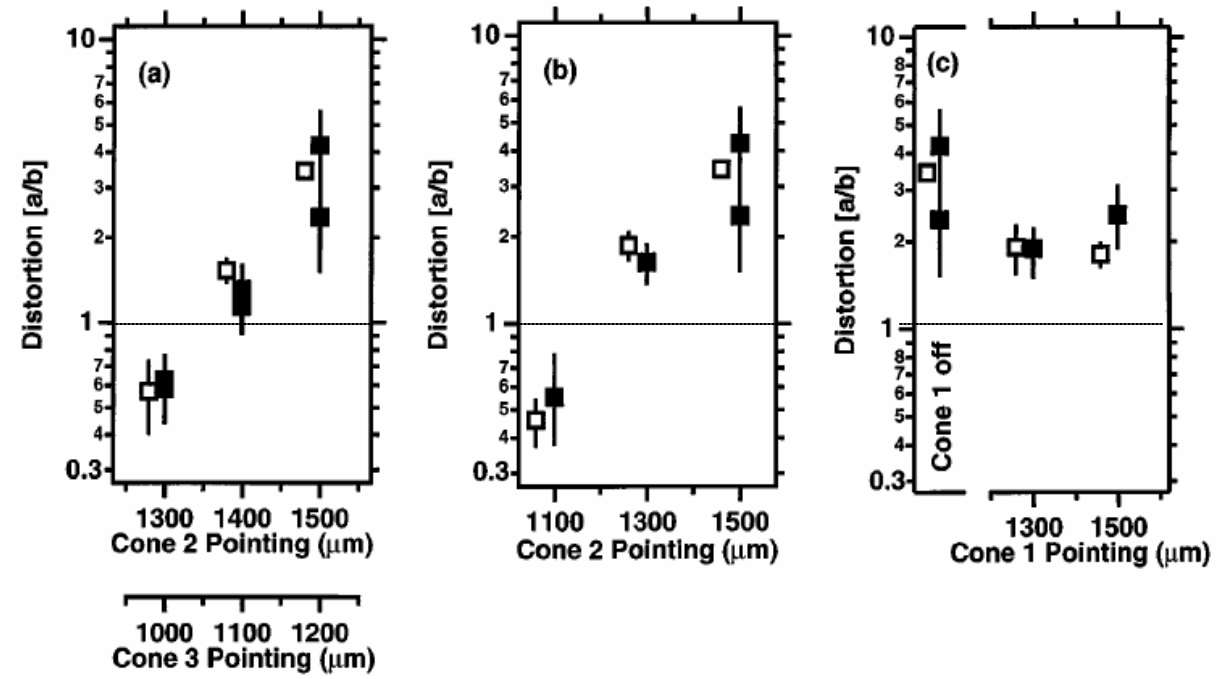

Figure 7. Distortion as a function of beam pointing for experiment series (a) in which beam Cones 2 and 3 formed a single ring on each side of the hohlraum, (b) in which the pointing of Cone 2 was varied while that of Cone 3 remained fixed at 1200 μm, and (3) in which Cone 1 was added while Cones 2 and 3 remained fixed at 1500 μm and 1200 μm, respectively. The uncertainty in the data (solid symbols) was determined by analyzing multiple images and contours on the same experiment. The uncertainty from the LASNEX simulations (open symbols, slightly offset) represents the range of calculations obtained from LLNL and LANL versions of LASNEX. (From Murphy *et al.* 1998).